Hyperon Production in Interactions of 2.7-GeV/c Antiprotons on Protons*

G. P. Fisher, V. Domingo, Å. J. Eide, J. von Krogh, L. Marshall Libby, and R. Sears

University of Colorado, Boulder, Colorado

AND

D. Bohning, W. Kernan, and L. Schroeder

Iowa State University, Ames, Iowa

(Received 2 March 1967)

We have measured the cross sections for hyperon production in 2.7-GeV/c $\bar{p}p$ interactions. The values obtained are:

$\sigma(\bar{\Lambda}\Lambda) = 113 \pm 15\ \mu b, \sigma(\bar{\Sigma}^0\Lambda) + \sigma(\bar{\Lambda}\Sigma^0) = 66 \pm 13\ \mu b,$

$\sigma(\bar{\Sigma}^0\Sigma^0) < 15\ \mu b, \sigma(\bar{\Xi}^0\Xi^0) = \le 2.8\ \mu b\ (90\% \text{ confidence})$

$\sigma(\bar{\Sigma}^-\Sigma^+) = 30.7 \pm 9.4\ \mu b, \sigma(\bar{\Sigma}^+\Sigma^-) = 1.0 \pm 5.4\ \mu b$ (large error resulting from subtraction),

$\sigma(\bar{\Xi}^+\Xi^-) = \le 1.8\ \mu b\ (90\% \text{ confidence}), \sigma(\bar{\Lambda}\Lambda\pi^0) = 65 \pm 25\ \mu b,$

$\sigma(\bar{\Sigma}^-\Lambda\pi^+ + \text{c.c.}) = 25.9 \pm 10.1\ \mu b, \sigma(\bar{\Sigma}^-\Sigma^0\pi^+ + \text{c.c.}) = 2.9 \pm 2.9\ \mu b$ (one event),

$\sigma(\bar{\Sigma}^+\Lambda\pi^- + \text{c.c.}) = 6.6 \pm 3.9\ \mu b, \sigma(\bar{\Sigma}^+\Sigma^0\pi^- + \text{c.c.}) = 3.7 \pm 2.6\ \mu b,$

$\sigma(\bar{\Sigma}^-\Sigma^+\pi^0) = \le 3.6\ \mu b\ (90\% \text{ confidence}), \sigma(\bar{\Lambda}\Lambda\pi^+\pi^-) = 3 \pm 2\ \mu b,$ and $\sigma(\Lambda K^+\bar{p}) = 2.3 \pm 2.3\ \mu b$ (one event). The ratios of the cross sections for the two-body final states have been compared with predictions of SU_3 and are in good agreement with the process being dominated by the exchange of an antisymmetric octet in the t channel. The angular distributions of $\bar{\Lambda}\Lambda$, $\bar{\Sigma}^-\Sigma^+$, and $\bar{\Lambda}\Lambda\pi^0$ final states clearly show the peripheral nature of these interactions. The differential cross section data for the interaction $\bar{p}p \rightarrow \bar{\Lambda}\Lambda$ have been compared with parametric equations and three absorption models. Good fits to the data have been achieved with each of these equations or models.

I. INTRODUCTION

THE total and differential cross sections for 2.7 GeV/c $\bar{p}$ on $p \rightarrow \bar{Y}Y$ with or without pions have been studied in order to learn more about their production mechanisms. The differential cross sections (t dependence) at this energy are helpful in testing various models of particle exchange and absorption. The ratios of the total cross sections at our energy are compared with predictions of SU_3 and are in good agreement with the assumption that all of the two-body final-state processes are dominated by exchange of an antisymmetric octet in the t channel.

The s dependence of these interactions is seen by comparing our data with those of other investigators at antiproton laboratory momenta of 1.6, 2.0, 3.0, 3.25, 3.6, 3.7, 4.0, 5.7, and 6.9 GeV/c,[1-5] for the two- and three-body final-state cross sections.

In the three- and four-body final states we have looked for resonances, structure in the angular distributions, and total cross sections.

[1] J. Button, P. Eberhard, G. R. Kalbfleisch, J. E. Lannutti, G. R. Lynch, B. C. Maglić, M. L. Stevenson, and N. H. Xuong, Phys. Rev. 121, 1788 (1961).
[2] B. Musgrave, G. Petmezas, L. Riddiford, R. Böck, E. Fett, B. R. French, J. B. Kinson, Ch. Peyrou, M. Szeptycka, J. Badier, M. Bazin, L. Blaskovic, B. Equer, J. Huc, S. R. Borenstein, S. J. Goldsack, D. H. Miller, J. Meyer, D. Revel, B. Tallini, and S. Zylberajch, Nuovo Cimento 35, 735 (1965).
[3] C. Baltay, J. Sandweiss, H.D. Taft, B. B. Culwick, J. K. Kopp, R. I. Louttit, R. P. Shutt, A. M. Thorndike, and M. S. Webster, Phys. Rev. 140, B1027 (1965).
[4] R. K. Böck, W. A. Cooper, B. R. French, J. B. Kinson, R. Levi-Setti, D. Revel, B. Tallini, and S. Zylberajch, Phys. Letters 17, 166 (1965).
[5] C. Y. Chien, J. Lach, J. Sandweiss, H. D. Taft, N. Yeh, Y. Oren, and M. Webster, Phys. Rev. 152, 1171 (1966).

Because of the small fiducial volume in which we must see both production and decay of the hyperons, we collected insufficient data to measure lifetimes or masses of the hyperons to accuracies of Chien et al.[5] Also, because of the very peripheral nature of the interactions with antihyperons predominantly going forward with large energy in the laboratory, we have very different detection efficiencies and measurement accuracies for hyperons and antihyperons. Therefore, we cannot take full advantage of the charge-conjugation invariance of the interactions.

II. DATA COLLECTION AND REDUCTION

91 000 pictures of the interactions of 2.7-GeV/c antiprotons on protons were taken in the Brookhaven National Laboratory 20-inch Liquid Hydrogen Bubble Chamber.

The antiprotons were produced in the 30-GeV Alternating Gradient Synchrotron, and after two stages of electrostatic separation,[6] the beam was better than 99% pure antiprotons as determined from a δ-ray analysis. The beam momentum[7] was 2700 MeV/c with half width at half-maximum of 70 MeV/c.

The odd numbered rolls of film taken at the bubble

[6] C. Baltay, H. N. Brown, J. Sandweiss, J. R. Sanford, M. S. Webster, and S. S. Yamamoto, Nucl. Instr. Methods 20, 37 (1963).
[7] We do not fully understand why the Λ and Σ^0 masses are larger than expected. In a study of two-prong events (to be published) the average unfitted beam momentum appears to drift by about 30 MeV/c from roll to roll (about 1000 events per roll). By reducing the beam momentum used in fitting these events from 2700 to about 2665 MeV/c, the Λ and Σ^0 masses can be made to agree with 1115 and 1190 MeV/c^2, respectively. Another possible explanation may come from our difficulty in locating the zero-prong production vertex accurately.

chamber (47 200 frames) were scanned and measured at the University of Colorado and the even numbered rolls (44 100 frames) at Iowa State University. The scanning efficiency for Λ and charged Σ decays within the acceptance limits is estimated to be 98%.

Physics graduate students examined each of the events displaying a vee and discarded events with clearly defined electron or positron tracks forming the vee. The criterion for identifying electron and positron tracks is: a track is from an electron or positron if the ionization density of the track is less than twice that for minimum ionization and the momentum projected on the viewing plane is less than 100 MeV/c as determined by the use of an appropriate template. This criterion is independent of the dip of the track for dips between 0° and about 60°.

Those events which were not discarded for having electrons or positrons in the vees were measured on conventional manually operated measuring machines with Datex brush encoders. The measured events were processed by the DATPRO–GUTS reconstruction and kinematic fitting routines.

Events were rejected if either the production or decay (vee or kink) vertex was not within the same fiducial volume defined by: $4.0 \leq x \leq 15.5$ in., $2 \leq y \leq 8$ in., $2 \leq z \leq 8$ in. The bubble chamber is $20 \times 10 \times 10$ in. We have defined one vertex of the chamber to be the origin of a right-handed coordinate system with axes along the edges of the chamber. The x axis is nearly along the beam direction, the y axis along the gravity direction, and the z axis is along the magnetic field and parallel to the optical axes of the cameras.

Acceptance limits were placed on the azimuthal angle [$\tan(az) \equiv p_y/p_x$] and the dip angle [$\sin(\text{dip}) \equiv p_z/p$] of the beam track as a function of the x coordinate of the production vertex (X).

$$az \text{ (degrees)} = -1.61 - 0.29X \text{ (in.)} \pm 1.4$$

$$\text{dip (degrees)} = +0.5 \pm 4.0.$$

The final states of the interactions were determined by a comparison of the observed ionization densities of the tracks with those expected for a given fit according to GUTS.

III. NEUTRAL TWO-BODY FINAL STATES

A. Data

The interactions $\bar{p}p \to \bar{\Lambda}\Lambda$, $\bar{\Lambda}\Sigma^0$, $\bar{\Sigma}^0\Lambda$, $\bar{\Sigma}^0\Sigma^0$, and $\bar{\Xi}^0\Xi^0$ are among the zero-prong-one- (or two-) vee events in which the vees are either Λ or $\bar{\Lambda}$ decays. Because of the peripheral nature of these interactions the $\bar{\Lambda}$ is normally produced with about 2000 MeV/c momentum and very small opening angle in the laboratory system. These $\bar{\Lambda}$ decays can be measured with sufficient accuracy to establish the fact that they are $\bar{\Lambda}$ decays; however, the computed momentum of the $\bar{\Lambda}$ has large errors. Therefore, for all practical purposes, visible $\bar{\Lambda}$ decays

were not used in reconstruction of a production event except when accompanied by a visible Λ or $\Sigma^{\pm}$ decay.

Because of the relatively wide spacing between bubbles in minimum ionizing tracks, when the vee from the Λ decay is close to the vertex where the Λ is produced, the scanners are likely to interpret many of the zero-prong–one-vee events as two-prong events. Therefore, we have discarded all Λ events in which the distance between the production vertex (the last bubble of the incoming beam track) and the decay vertex of the Λ is less than 0.25 in. in real space.

To compute the cross sections each event is weighted by the inverse of the probability that the Λ will decay at least 0.25 in. from the production vertex; but within the fiducial volume; and that the Λ decays into $\pi^- p$ which yields visible tracks. This weight is

$$W = 1.5/(e^{-t_{\min}/\tau} - e^{-t_{\max}/\tau}),$$

where

$$t/\tau = (mc^2/Pc)(L/\tau c).$$

We have taken the rest mass (m) of the Λ to be 1115.44 MeV/c^2 and the mean proper lifetime (τ) of the Λ to be 2.6×10^{-10} sec. P is the laboratory momentum of the Λ; $L_{\min} = 0.25$ in.; and $L_{\max}$ is the distance along the Λ direction, between the production vertex and the boundary of the fiducial volume. The factor 1.5 in the weight is the inverse of the probability of the Λ decaying to $\pi^- p$. The 60 events used to determine the angular distribution of $\bar{p}p \to \bar{\Lambda}\Lambda$ have an average weight of 2.17 with almost all weights between 1.7 and 2.2 (6 events have weights between 2.2 and 2.9 and one event each with 3.47, 4.49, and 8.59).

The missing mass has been computed for each of the 113 zero-prong-one-vee events for which the vee has been identified as a Λ decay ($\bar{p}p \to \Lambda + $ missing mass). All events with missing mass less than 1150 MeV were accepted as uniquely identified $\bar{p}p \to \bar{\Lambda}\Lambda$ events. The kinematic fitting program (GUTS) has been used on all events containing a Λ. The 60 events selected on the basis of missing mass are found to have good kinematic fits to $\bar{p}p \to \bar{\Lambda}\Lambda$, although some of these events (with missing mass near 1150 MeV/c^2) are also consistent with other hypotheses, notably $\bar{p}p \to \Lambda\bar{\Sigma}^0$. This ambiguity has negligible effect on the shape of the $\bar{p}p \to \bar{\Lambda}\Lambda$ angular distribution because the angular distributions are similar. The angular distribution of $\bar{p}p \to \bar{\Lambda}\Lambda$ events selected in this manner is plotted in Figs. 1–5.

In order to estimate total cross sections of the final states, we made a Gaussian ideogram of the missing mass of all 113 Λ events. (See Fig. 6.) The error of the missing mass due to estimated measurement errors was computed by GUTS and used to determine the width of each of the Gaussians in the ideogram. This ideogram[7] was then fitted by the sum of a Gaussian peaked at 1120 MeV/c^2 ($\bar{\Lambda}\Lambda$), a Gaussian peaked at 1200 MeV/c^2 ($\bar{\Sigma}^0\Lambda$), and, to take into account $\bar{\Lambda}\Sigma^0$ processes, a rectangle with bounds at 1140 and 1320 MeV/c^2. This five-

FIG. 1. Angular distribution of $\bar{p}p \to \bar{\Lambda}\Lambda$ interaction events. The weighted number of events per $\Delta \cos\theta = 0.05$ versus $\cos\theta$ where θ is the angle in the c.m. system between the p and the Λ (60 events).
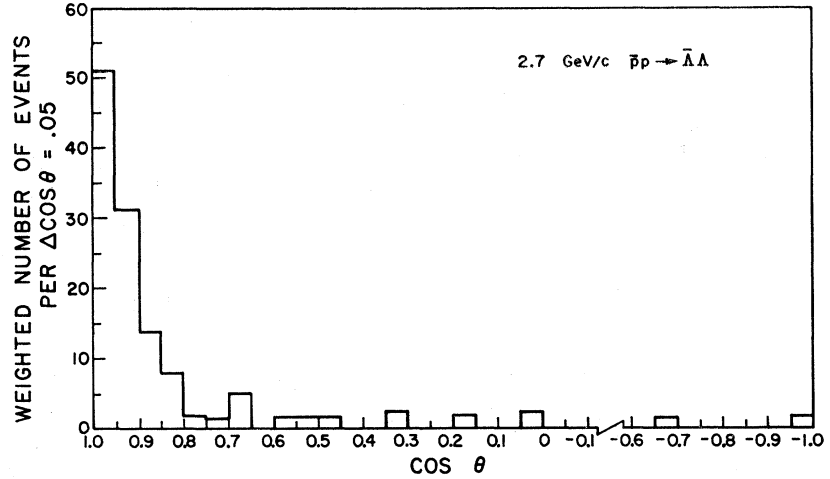
parameter fit was made by finding the values of the parameters (amplitude and width of each Gaussian and amplitude of the rectangle) which gives the least-squares deviation from the ideogram of the data. The total area under the parametric curve is constrained to be the weighted number of events in the data which have missing mass less than 1320 MeV/c^2. One weighted event is equivalent to 0.91 μb. Using the parameters which give the best fit to the Gaussian ideogram and correcting the cross section of $\bar{\Sigma}^0\Lambda + \bar{\Lambda}\Sigma^0$ for the overlap with $\bar{\Sigma}^0\Sigma^0$ and

$\bar{\Lambda}\Lambda\pi^0$ events, we obtain $\sigma(\bar{p}p \to \bar{\Lambda}\Lambda) = 113\pm15$ μb, $\sigma(\bar{p}p \to \bar{\Sigma}^0\Lambda) + \sigma(\bar{p}p \to \bar{\Lambda}\Sigma^0) = 66\pm13$ μb, and

$$\sigma(\bar{p}p \to \bar{\Sigma}^0\Sigma^0) < 15 \ \mu\text{b}.$$

No events were found which were consistent with being $\bar{p}p \to \bar{\Xi}^0\Xi^0$. These events would be zero-prong–one-(or two-) vee final states. The visible Λ or $\bar{\Lambda}$ would originate from the Ξ^0 or $\bar{\Xi}^0$. Since Ξ^0 has a lifetime of 3×10^{-10} sec, it will normally have moved a few centi-
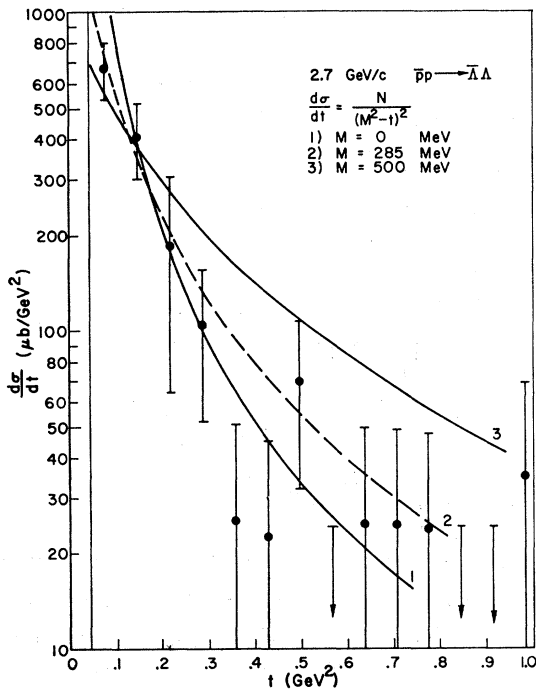
FIG. 2. Differential cross section of 60 events of $\bar{p}p \to \bar{\Lambda}\Lambda$ interactions plotted as a function of four-momentum transfer squared (t). Error bars are statistical errors. Error bars with arrows indicate no events. Curves represent the parametric equation $d\sigma/dt = N/(M^2-t)^2$ for $M = 0$, 285, and 500 MeV. Values of N are arbitrary scale factors.
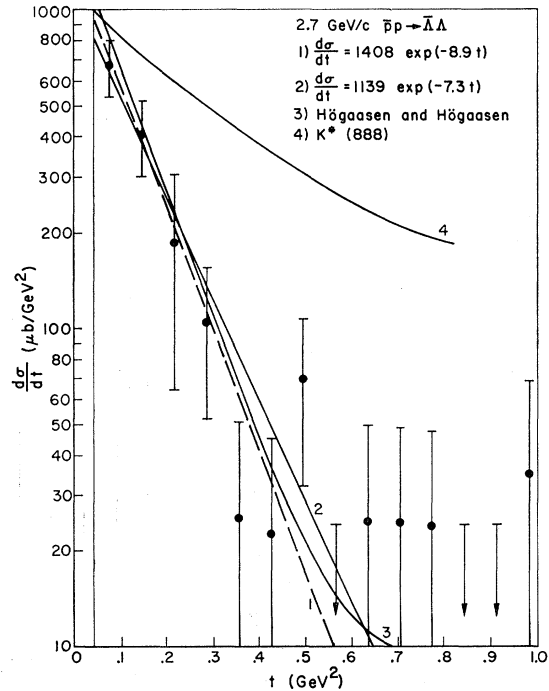
FIG. 3. Differential cross section of 60 events of $\bar{p}p \to \bar{\Lambda}\Lambda$ interactions versus four-momentum transfer squared (t). Error bars are statistical errors. Error bars with arrows indicate no events. Curves 1 and 2 are exponentials; curve 3 is the prediction of Högaasen and Högaasen using a distorted wave Born approximation with K^*(888) exchange. Curve 4 is a simple Born approximation with exchange of K^*(888) with arbitrary scale factor.
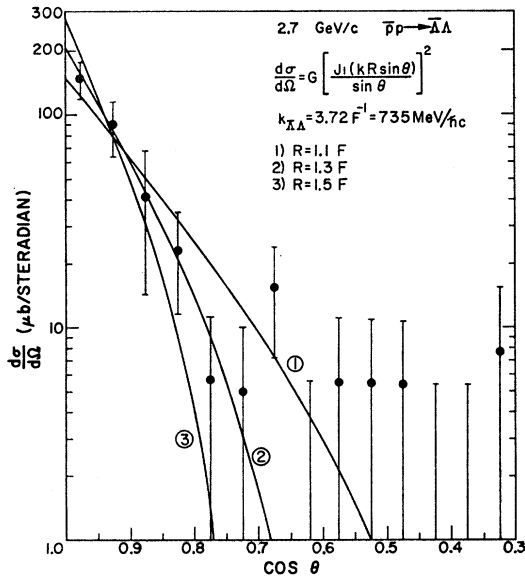
Fig. 4. Differential cross section of 60 events of $\bar{p}p \to \bar{\Lambda}\Lambda$ interactions plotted as a function of $\cos\theta$ where θ is the c.m. angle between the $\bar{p}$ and the Λ. Error bars are statistical errors. Error bars without dots indicate no events. Three curves shown represent reacting disks with radii 1.1, 1.3, and 1.5 F.
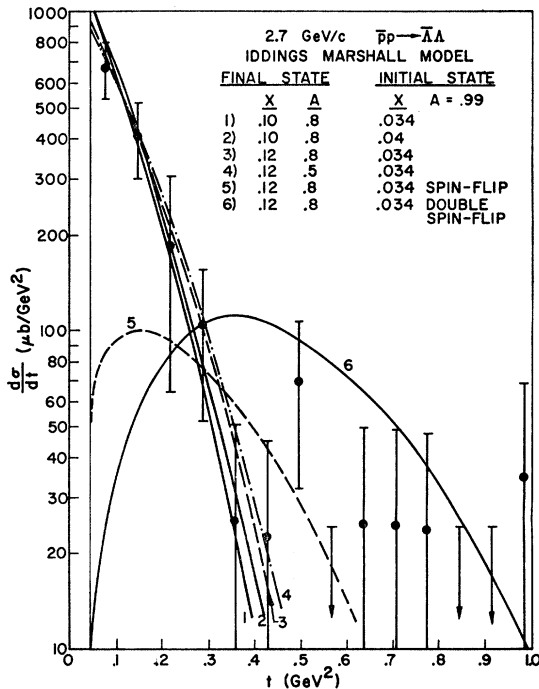
Fig. 5. Differential cross section of 60 events of $\bar{p}p \to \bar{\Lambda}\Lambda$ interactions versus four-momentum transfer squared (t). Error bars are statistical errors. Error bars with arrows indicate no events. Curves 1–6 have been computed from droplet model of Iddings and Marshall for various parameters X and A for the $\bar{\Lambda}\Lambda$ state. X in the initial state has been varied slightly to provide for present experimental uncertainties in $\bar{p}p$ differential elastic scattering. Curves 5 and 6 are single-spin-flip and double-spin-flip contributions predicted by the model. Each of curves 1 through 6 has a different and arbitrary scale factor [A dimensionless, X in GeV²].

meters from where it was produced to where it decays. The Ξ^0 and $\bar\Xi^0$ are kinematically constrained at production to be within $\sim 10°$ of the direction of the incident antiproton. We have, therefore, examined all of the Λ decays in our data, including vees with no production vertex along their line of flight, to see if any passed within a few centimeters of a zero-prong antiproton vertex. Those that were found were not kinematically consistent with the hypothesis. If one event had been found with weight of 1.5, the cross section would be 1.4 ± 1.4 μb.

B. Discussion

Attempts have been made by several authors to fit the available data to models with simple $K(0^-)$ or $K^*(1^-)$ exchange,[8,9] Reggeized $K^*(1^-)$ exchange,[9,10] mixtures of K and K^* coupled by $\bar{U}_{12}$ symmetry,[11] as well as various absorption models.[12,13] (None of these models seems to satisfactorily predict both the s and t dependence of the $\bar{p}p \to \bar\Lambda\Lambda$ cross sections.) Regge poles[10] are able to predict the s dependence (see Fig. 11a). The absorption models of Högaasen and Högaasen[12] and Iddings and Marshall[13] have been used to fit the t dependence. We shall now discuss various parametrizations and models which were used to fit these data.

1. Propagator

The first parametric equation used to fit the differential cross section of $\bar{p}p \to \bar\Lambda\Lambda$ resembles a simple propagator of mass M

$$d\sigma/dt = N/(M^2+t)^2,$$

where $d\sigma/dt$ is the differential production cross section as a function of two adjustable parameters N and M and the invariant four-momentum transfer squared t ($t = 1.437 - 1.392 \cos\theta$, where t is in GeV⁻² and θ is the angle between the $\bar{p}$ and the Λ in the c.m. of the $\bar{p}p$ system). N is merely a normalization factor. The fitting was done in two ways:

(a) A least χ^2 [14] fit was made to the mean differential cross section in each bin (Each bin is $\cos\theta = 0.05$ wide). The best fit [$\chi^2 = 0.8$ for 2 degrees of freedom] is $M = 285 \pm 30$ MeV. Fits to the first 3, 4, 7 consecutive bins yield values of M which are 316, 285, 253 MeV,

[8] H. D. D. Watson, Nuovo Cimento **29**, 1338 (1963).

[9] C. H. Chan, Phys. Rev. **133**, B431 (1964).

[10] D. P. Roy, Phys. Rev. **146**, 1218 (1966); also, private communications.

[11] H. D. D. Watson and J. H. R. Migneron, Phys. Letters **19**, 424 (1965).

[12] H. Högaasen and J. Högaasen, Nuovo Cimento **40**, 560 (1965); (private communication).

[13] C. Iddings and L. Marshall, Phys. Rev. **154**, 1522 (1967).

[14] Each of the curves has been fitted by minimizing the χ^2, where

$$\chi^2 = \sum_i \frac{(M_i - T_i)^2}{T_i \bar{w}}.$$

M_i is the measured weighted number of events in bin i. T_i is the theoretical weighted number of events in bin i, and $\bar{w}$ is the average weight of an event. This χ^2 assumes a Poisson statistical distribution of events in each bin.

FIG. 6. Gaussian ideogram of 113 events with no prongs at the production vertex and a visible Λ decay, the missing mass and errors were computed by GUTS. The fitted curve is the sum of two Gaussians and a rectangular distribution. The values of the 5 adjustable parameters are given in the figure. ($A_{1,2,3}$ has units of events per MeV, $\sigma_{1,2}$ has units MeV, and the differential cross section has units of events per MeV.)
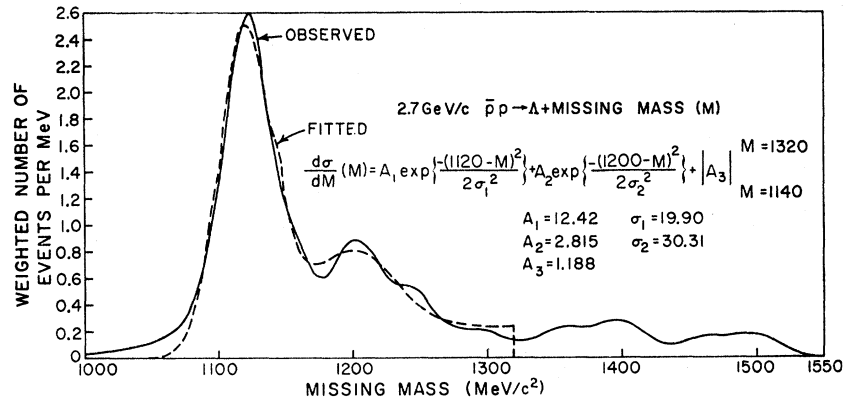
respectively. The results of this calculation with $M = 0$, 285, and 500 MeV are presented in Fig. 2.

(b) For rapidly varying functions it is better to integrate the parametric equation over each bin of width Δ to obtain the mean differential cross section for that bin. This is in closer correspondence to the data. Thus,

$$\sigma(t) = \int_t^{t+\Delta} \frac{N}{(M^2+t)^2} dt = \frac{N\Delta}{(M^2+t)(M^2+t+\Delta)}.$$

M is easily obtained by taking the ratio of two adjacent bins

$$\sigma(t)/\sigma(t+\Delta) = 1 + [2\Delta/(M^2+t)].$$

Each pair of bins gives a value of M. The first two bins give $M \simeq 420$ MeV, and all the remaining pairs of adjacent bins give $M \simeq 0$ MeV. This small value for the "propagator" mass is an indication of the strongly peripheral nature of the interaction.

2. Exponential

Another parametrization, an exponential forward scattering cross section, was used to fit the data

$$d\sigma/dt = A e^{-Bt}.$$

Fits to the first 3, 4, 7 bins yield values of $A = 1384$, 1408, 1139 μb/GeV^2 and $B = +8.76$, 8.93, 7.32 GeV^{-2}, respectively. Two of these fitted curves are presented in Fig. 3. The fit with four bins of data is the best fit to the forward peak and has $\chi^2 = 0.2$ for two degrees of freedom and $d\sigma/dt = [(1400\pm210)\exp(-8.9\pm1.6)t] \mu$b/GeV^2. It is useful to note that the $\bar{p}p$ differential elastic scattering cross section at this energy (to be published) has logarithmic derivative $B \simeq 13$ GeV^{-2}.

3. Reacting Disk

The first of the three absorption models to be discussed is that of a black disk of radius R which totally absorbs the antiprotons falling incident upon it. A certain fraction (G/R^2) of these absorbed antiprotons reacts to produce a $\bar{\Lambda}\Lambda$ final state which is radiated coherently and uniformly from the disk. The factor G/R^2 may be

thought of as an emissivity for this reaction. This model gives a differential cross section of the form

$$\frac{d\sigma}{d\Omega} = G \left| \frac{J_1(kR \sin\theta)}{\sin\theta} \right|^2.$$

We have fit this function to the data in the forward peak only; $\hbar k$ is the c.m. momentum of the $\bar{\Lambda}$, θ is the c.m. angle between the incident $\bar{p}$ (the normal to the disc) and the $\bar{\Lambda}$. The best fit is for $R = 1.3$ F and $G = 36$ μb. This curve is plotted in Fig. 4 along with curves for $R = 1.3 \pm 0.2$ F. The emissivity $(G/R^2) = 2.14 \times 10^{-3}$ and the area $\pi R^2 = 53.2$ mb. Elastic scattering of $\bar{p}p$ may be described by diffraction from a totally absorbing (black) disk of radius R. Since the radii for $\bar{p}p$ elastic scattering at 3.0^{15} and 3.28^{16} GeV/c are 1.4 F and 1.3 F, respectively, the $\bar{p}p \to \bar{\Lambda}\Lambda$ interaction volume must be the same size as the elastic scattering volume. It should be noted that at the energy of this experiment the c.m. wavelengths are 1.3 F for the $\bar{p}$ and 1.7 F for the $\bar{\Lambda}$ which are both quite close to the interaction radius $R = 1.3$ F.

4. Distorted-Wave Born Approximation

The absorption model of Högaasen and Högaasen[12] makes use of a distorted-wave Born approximation with the exchange of $K^*(888)$ in the t channel in a manner which is very similar to that used by Gottfried and Jackson[17] in other types of interactions. Högaasen and Högaasen have included both vector and tensor coupling of the K^* to the baryon vertex. They have been kind enough to use their model to compute the differential cross section for $\bar{p}p \to \bar{\Lambda}\Lambda$ at 2.7 GeV/c. The coupling constants are the same as were used at 3.0

[15] Y. Goldschmidt-Clermont, M. Guinea, T. Hofmokl, R. Lewisch, D. R. O. Morrison, M. Schneeberger, and S. de Unamuno, in *Proceedings of the 1962 Annual International Conference on High-Energy Nuclear Physics at CERN*, edited by J. Prentki (CERN, Geneva, 1962), p. 84.

[16] T. Ferbel, J. Sandweiss, H. D. Taft, M. Gailloud, T. W. Morris, R. M. Lea, and T. E. Kalogeropoulos, in *Proceedings of the 1962 Annual International Conference on High-Energy Nuclear Physics at CERN*, edited by J. Prentki (CERN, Geneva, 1962), p. 76.

[17] K. Gottfried and J. D. Jackson, Nuovo Cimento **34**, 735 (1964).

GeV/c; viz. $c_i = c_f = 1.0$, $A = 16$ GeV^{-2}, $g^2_{K*N\Lambda}/4\pi = 3.7$, and $g_T = g_V$ in the notation of Ref. 12. The prediction of this model is in excellent agreement with our data (Fig. 3). For $t < 0.5$ GeV^2 this curve is an exponential with the same slope as our best fit, viz. $B = 8.9$ GeV^{-2}. The effect of taking absorption of the low partial waves into account may be seen by comparing this curve with that for a simple Born approximation with no absorption[8] [see curve marked $K*(888)$]. The difficulties that this model has in predicting the proper s dependence of the cross section are discussed in Ref. 12.

5. Droplet Model

The absorption model of Iddings and Marshall[13] is a distorted-wave droplet model. The absorptive elastic-scattering part of the scattering amplitude (distorted wave) is computed in the same manner as Högaasen and Högaasen[12] and Yang and Byers[18] with the exception that the final state ($\bar{\Lambda}\Lambda$) parameters determining the Gaussian shape of the optical density are not assumed to be the same as those of the initial state ($\bar{p}p$), but instead are determined by computer search to fit the experimental data. Where Högaasen and Högaasen[12] use the Born approximation for exchange of a $K*(888)$ meson, Iddings and Marshall use a term proportional to the geometric mean of the $\bar{\Lambda}$ and $\bar{p}$ phase shifts for absorptive elastic scattering of the initial and final states. Applying this model to $\bar{p}p \rightarrow \bar{\Lambda}\Lambda$, we have computed the curves presented in Fig. 5 using different input (A_p, X_p) and ouput (A_l, X_l) parameters in the notation of Ref. 13. These curves are in excellent agreement with the data. The curves are reasonably insensitive to the input parameters A_p and X_p, as well as A_l. The best fit to the data is with $A_p = 0.99$, $X_p = 0.034$ GeV^2, $A_l = 0.8 \pm 2$, and $X_l = 0.10 \pm 0.02$ GeV^2.

With these values of A_l and X_l, this model predicts a total cross section of 20 ± 10 mb for Λ's interacting with $\bar{\Lambda}$'s.

IV. CHARGED TWO-BODY FINAL STATES

A. Data

Since most Σ^+ and Σ^- particles produced by $\bar{p}p$ interactions are expected to decay within the fiducial volume, we have looked for $\bar{\Sigma}^-\Sigma^+$ and $\bar{\Sigma}^+\Sigma^-$ final states in events with two prongs at the production vertex and with a kink (Σ decay) on each prong. The 40 events of this type found in scanning the film were measured three times each, in order to make reliable identifications of the short Σ tracks. Eleven of the events have one or more vertices (production or decay) outside of the fiducial volume and were rejected. Three other events are unmeasurable: one event has a kink which is only three bubbles (0.12 in.) from the production vertex, and each of the other two events has a kink involving a

---
[18] N. Byers and C. N. Yang, Phys. Rev. **142**, 976 (1966).

TABLE I. Summary of $\bar{Y}^\mp Y^\pm$ data.

	Unique $\bar{\Sigma}^-\Sigma^+$	Ambiguous	Total
Number of events	11	6	17
Weighted number[a]	25.3±7.8	9.6±4.0	34.9±8.7
Cross section (μb)	23.0±7.1	8.7±3.6	31.7±7.9

$\sigma(\bar{\Sigma}^-\Sigma^+) = \frac{4}{3}\sigma(\text{unique}) = 30.7 \pm 9.4$ μb

$\sigma(\bar{\Sigma}^+\Sigma^-) = \sigma(\text{ambiguous}) - \frac{1}{3}\sigma(\text{unique}) = 1.0 \pm 5.4$ μb.

[a] See Refs. 19 and 20.

change of direction of the tracks which is so slight that the location of the decay vertex is very poorly defined thus preventing identification of the decaying particle.

After the remaining 26 events were run through the GUTS kinematical fitting program which tried to fit each kink to the decay of a μ, π, K, Σ, and Ξ, nine events were found to involve meson decays.

The 17 events remaining were identified as $\bar{\Sigma}^-\Sigma^+$ or $\bar{\Sigma}^+\Sigma^-$ final states, none consistent with $\bar{\Sigma}^\mp\Sigma^\pm\pi^0$. One event with a weight of two corresponds to a cross section of 1.8 ± 1.8 μb. The kinematic fit ambiguity at the production vertex between $\bar{\Sigma}^-\Sigma^+$- and $\bar{\Sigma}^+\Sigma^-$-final states is removed if either of the Σ's decays, because at these energies, ionization density distinguishes a proton from a pion. Since the Σ^+ decays into $p\pi^0$ half of the time, and into π^+n the other half of the time, 75% of the final state $\bar{\Sigma}^-\Sigma^+$ will have decay products containing proton or antiproton or both and are thereby uniquely distinguished from $\bar{\Sigma}^+\Sigma^-$ which do not decay into p or $\bar{p}$. The remaining 25% of the $\bar{\Sigma}^-\Sigma^+$ events along with all of the $\bar{\Sigma}^+\Sigma^-$ events remain ambiguous.

After examining the ionization of the tracks, we have found 11 unique $\bar{\Sigma}^-\Sigma^+$ events and six events ambiguous between $\bar{\Sigma}^-\Sigma^+$- and $\bar{\Sigma}^+\Sigma^-$-final states. These events have
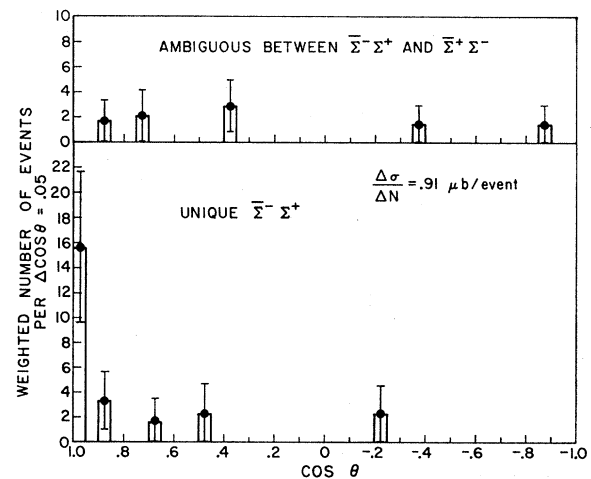
FIG. 7. Angular distribution of $\bar{p}p \rightarrow \bar{Y}^\mp Y^\pm$ as a function of $\cos\theta$, where θ is the c.m. angle between the $\bar{p}$ and the $\bar{\Sigma}^-$. The lower curve is of 11 events uniquely $\bar{p}p \rightarrow \bar{\Sigma}^-\Sigma^+$. The upper curve is of 6 events ambiguous between $\bar{\Sigma}^-\Sigma^+$ and $\bar{\Sigma}^+\Sigma^-$, assuming all events to be $\bar{p}p \rightarrow \bar{\Sigma}^-\Sigma^+$.

been weighted[19,20] to obtain the cross sections given in Table I. The angular distributions are plotted in Fig. 7 assuming all events to be $\bar{\Sigma}^-\Sigma^+$.

B. Discussion

The u-channel production (Fig. 8) of $\bar{\Sigma}\Sigma$ requires doubly strange double baryon exchange. If double charge exchange can be ruled out, then $\bar{\Sigma}^+\Sigma^-$ cannot be produced in the t channel although $\bar{\Sigma}^-\Sigma^+$ can. It is expected that $\bar{\Sigma}^+\Sigma^-$ is produced equally as often as $\bar{\Sigma}^-\Sigma^+$ in the s channel, in which case the cross section for producing a charged $\bar{\Sigma}\Sigma$ pair through the s channel is twice that for $\bar{\Sigma}^+\Sigma^-$. Supposing all graphs other than the s and t channels to be negligible, the remainder of the cross section for charged $\bar{\Sigma}\Sigma$ production is through the t channel. $[\sigma(s)=2.1\pm10.9$ μb and $\sigma(t)=29.7\pm7.9$ μb.]

The differential cross section of $\bar{\Sigma}^-\Sigma^+$ events in the t channel is expected to be peripheral with the $\bar{\Sigma}^-$ being nearly in the direction of the incident $\bar{p}$, consistent with the very sharp forward peak of the $\bar{\Sigma}^-$ angular production presented in Fig. 7, whereas production via the s channel is expected to have an isotropic distribution.
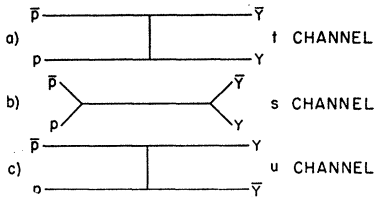
FIG. 8. Diagrams defining the t, s, and u channels.

Our data are consistent with no $\bar{\Sigma}^+\Sigma^-$ production and, therefore, pure $\bar{\Sigma}^-\Sigma^+$ production via the t channel.

No events of $\bar{p}p\rightarrow\bar{\Xi}^+\Xi^-$ were found in these data. One event with unit weight would correspond to a cross section of 0.9 ± 0.9 μb.

V. NEUTRAL THREE-BODY FINAL STATES

Among the events with zero prongs at the production vertex and two vees which are identified as a $\bar{\Lambda}$ and a Λ, there are ten events which have been identified as being

[19] The weights used here are the inverse of the probability that both sigmas decay between 0.15 in. from the production vertex and the boundary of the fiducial volume. All of the charged Σ's and $\bar{\Sigma}$'s have ranges sufficiently long to escape the fiducial volume. These weights for unique $\bar{\Sigma}^-\Sigma^+$ range from 1.25 to 1.84.

[20] It is very important to correct for losses due to decays with very small projected angular deviation between the Σ and the charged decay product. Since almost all of our sigmas have small dips, the correction is a function of Σ laboratory momentum and the smallest angular deviation that can be reliably observed in scanning and measuring. We believe that this angle is about 3° in our system. Assuming that the charged Σ decays isotropically in its center-of-mass system, for the charged decay product to have a projected kink angle (in the lab) of $<3°$, this weight is about 1.1 for $\Sigma^+\rightarrow\pi^+n$, whereas, for $\Sigma^+\rightarrow p\pi^0$ it ranges from 1 to 2 as the Σ^+ lab momentum goes from 600 to 2600 MeV/c. The corresponding weight range for a cutoff of 4° is 1.1 to 3.5 over the same range of momenta.
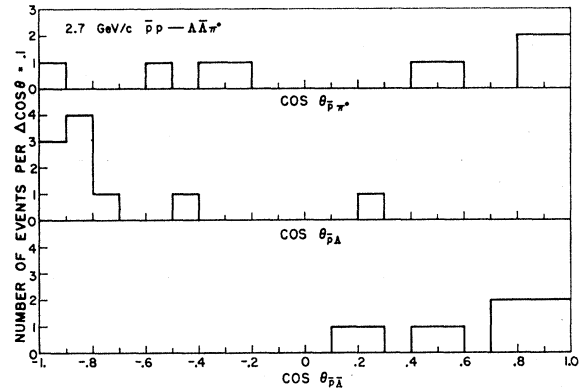
FIG. 9. Angular distribution of 10 events (not weighted) for $\bar{p}p\rightarrow\bar{\Lambda}\Lambda\pi^0$ versus, from top to bottom, the c.m. angle between the $\bar{p}$ and the π^0, Λ, and $\bar{\Lambda}$.

$\bar{p}p\rightarrow\bar{\Lambda}\Lambda\pi^0$. Each event has been weighted with the product of the individual weights for the Λ and $\bar{\Lambda}$ because we have accepted events only if both vees are visible and all vertices (production and both decays) are within the same fiducial volume. The total weight of these ten events is 71.3 ± 27.7 from which the cross section $(\bar{p}p\rightarrow\bar{\Lambda}\Lambda\pi^0)$ is determined to be 65 ± 25 μb.

Angular distributions of the Λ, $\bar{\Lambda}$, and π^0 shown in Fig. 9 indicate that this final state is probably produced peripherally.

The total c.m. energy of (2.7 GeV/c $\bar{p}p$) is 2670 MeV allowing production of Y^* resonances with masses up to 1555 MeV/c^2 of which the $Y_1^*(1385)$ is the only known resonance in this mass region with quantum numbers consistent with a pure $T=1$ state $(\Lambda\pi)$. The ten events in our data, plotted in Fig. 10, are too few to show evidence of Y^* production if it occurs.

In the Gaussian ideogram (Fig. 6) interactions of the form $\bar{p}p\rightarrow\Lambda\bar{Y}^*$ would appear at the mass of the $\bar{Y}^*$ It should be noted that this plot not only includes the invariant mass of $\bar{\Lambda}\pi$ combinations but also $\bar{\Sigma}^0\pi^0$, $\bar{\Lambda}\pi^0\pi^0$, $\bar{\Sigma}^0\pi^0\pi^0$, etc. Events of the form $\bar{p}p\rightarrow\bar{Y}^*+(\Sigma^0\rightarrow\Lambda+\gamma)$ contribute to the background because in this case, the invariant mass of the $\bar{Y}^*$ combines with the γ from the Σ^0 decay. $Y_1^*(1385)$ has been reported[2] to be present in 34% (20 ± 6 μb) of the $\bar{\Lambda}\Lambda\pi^0$ final states of 3.6- and 4.0-GeV/c $\bar{p}p$ interactions. Although our data show no evidence for $Y_1^*(1385)$, they are consistent with this report.
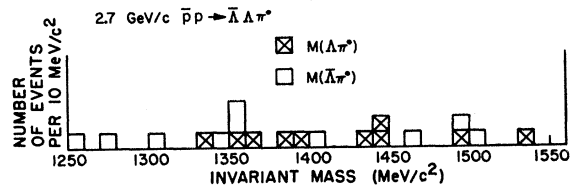
FIG. 10. Distribution of 10 events (not weighted) of the interaction $\bar{p}p\rightarrow\bar{\Lambda}\Lambda\pi^0$ versus invariant mass of $\bar{\Lambda}\pi^0$ and $\Lambda\pi^0$.
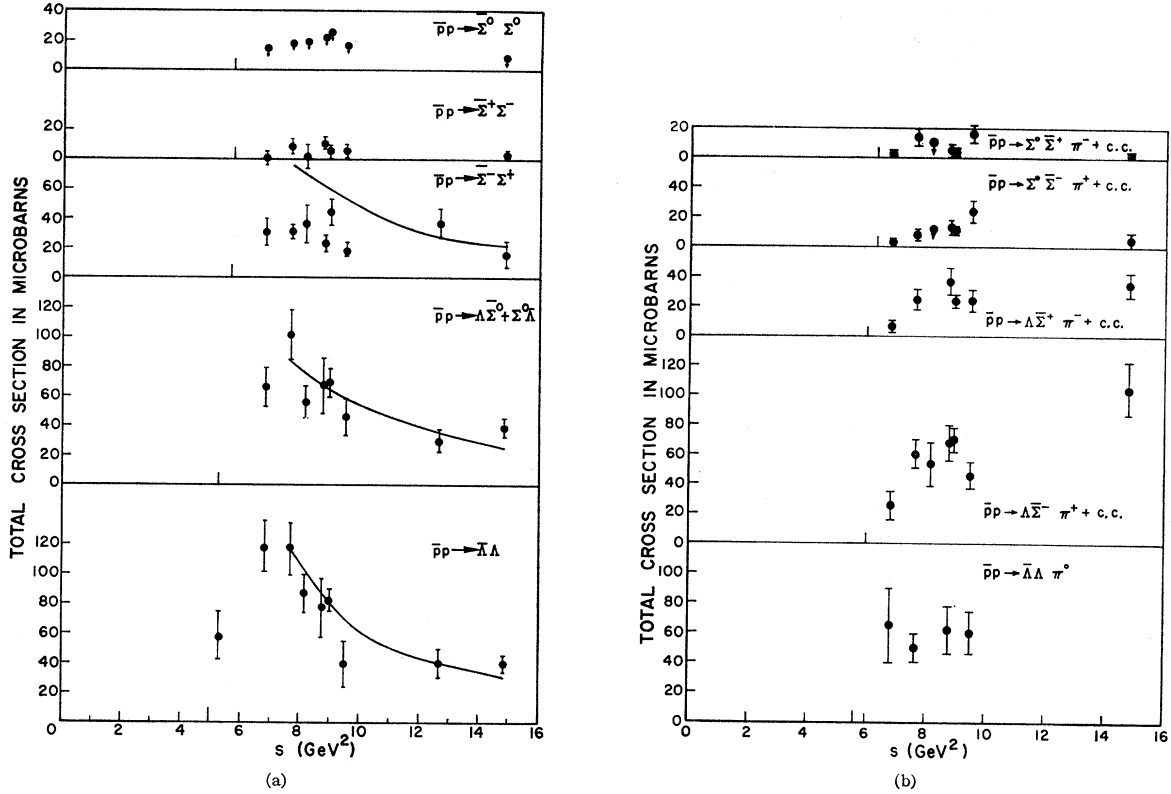
FIG. 11. Hyperon production cross sections (Refs. 1–5) in microbarns versus total c.m. energy-squared (s). $\bar{p}p$ interactions with anti-proton laboratory momenta of 1.61, 2.7, 3.0, 3.25, 3.6, 3.66, 4.0, 5.7, and 6.9 GeV/c have the following values of s: 5.28, 7.10, 7.67, 8.15, 8.77, 8.95, 9.52, 12.65, and 14.83 GeV², respectively. The curves for the final states $\bar{\Lambda}\Lambda$, $\bar{\Lambda}\Sigma^0+\bar{\Sigma}^0\Lambda$, and $\bar{\Sigma}^-\Sigma^+$ were computed by Roy (Ref. 10) using the exchange of $K^*(888)$-Regge pole. The thresholds are marked. The cross sections for reactions plus their charge conjugate are the sums of the individual cross sections.

VI. $Y^{\pm}\pi^{\mp}\bar{Y}^0$, $\bar{p}K^+Y^0$, $\bar{p}K^0Y^+$, AND CHARGE-CONJUGATE (c.c.) FINAL STATES

A careful study has been made of all events with two prongs at the production vertex, of which one prong has a kink (strange particle decay), and a vee decay of a neutral particle. All such events were considered whether or not the scanner thought that the neutral particle was produced at the production vertex, at the kink, or at neither. All scanned events surviving visual examination by physicists were measured and processed by the DATPRO–GUTS reconstruction and fitting programs. Events were rejected if one or more of the three vertices (production, kink, vee) was outside of the fiducial volume. A final criterion for acceptance was that the distance from the production vertex to the kink had to be greater than 0.15 in. and the distance from the production vertex to the vee had to be greater than 0.25 in.

A final sample of 14 acceptable events remained. These events are identified as follows:

$$\bar{p}+p \rightarrow \pi^+\bar{\Sigma}^-\Lambda \quad \text{(6 events)},$$
$$\bar{p}+p \rightarrow \pi^-\bar{\Sigma}^+\Lambda \quad \text{(4 events)},$$
$$\bar{p}+p \rightarrow \pi^-\Sigma^+\bar{\Lambda} \quad \text{(2 events)},$$
$$\bar{p}+p \rightarrow \pi^+\Sigma^-\bar{\Lambda} \quad \text{(2 events)}.$$

Due to the difficulty in measuring the charged decaying tracks, which are generally quite short, most of these events are ambiguous to the interchange of Λ or $\bar{\Lambda}$ with Σ^0 or $\bar{\Sigma}^0$, respectively. In the calculation of cross sections no correction has been made for one event that could not be completely measured due to secondary interactions. The events included have been weighted with escape corrections for both the neutral particle and the charged decaying track.[20]

TABLE II. Summary of hyperon production cross sections measured in 2.7-GeV/c $\bar{p}p$ interactions.

Final state	Cross section (μb)	
$\bar{\Lambda}\Lambda$	113 ± 15	
$\bar{\Sigma}^0\Lambda$+c.c.	66 ± 13	
$\bar{\Sigma}^0\Sigma^0$	<15	
$\bar{\Xi}^0\Xi^0$	≤2.8	(90% confidence)
$\bar{\Sigma}^-\Sigma^+$	30.7 ± 9.4	
$\bar{\Sigma}^+\Sigma^-$	1.0 ± 5.4	
$\bar{\Xi}^+\Xi^-$	≤1.8	(90% confidence)
$\bar{\Lambda}\Lambda\pi^0$	65 ± 25	
$\bar{\Sigma}^-\Lambda\pi^+$+c.c.	25.9 ± 10.1 } 28.8 ± 10.5	
$\bar{\Sigma}^-\Sigma^0\pi^+$+c.c.	2.9 ± 2.9	
$\bar{\Sigma}^+\Lambda\pi^-$+c.c.	6.6 ± 3.9 } 10.3 ± 4.7	
$\bar{\Sigma}^+\Sigma^0\pi^-$+c.c.	3.7 ± 2.6	
$\bar{\Sigma}^-\Sigma^+\pi^0$	≤3.6	(90% confidence)
$\Lambda K^+\bar{p}$	2.3 ± 2.3	(one event)
$\bar{\Lambda}\Lambda\pi^+\pi^-$	3 ± 2	(two events)

TABLE III. $SU(3)$ Clebsch-Gordan coefficients for $\bar{p}p \to$ 2-body final states in the cross channel (t channel). The amplitudes B_i are proportional to the t-channel amplitudes given by Tanaka in Ref. 21.

Final state	$\sigma(\mu b)$	Phase space	Test[a]	B_{8a}^2	B_{27}^2	B_{8s}^2	B_{10}^2	B_{as}^2	B_1^2
$\bar{\Lambda}\Lambda$	113 ± 15	1.23	9.0 ± 1.2	9	81	1	9	12	0
$\bar{\Sigma}^-\Sigma^+$	31 ± 9	1.0	3.0 ± 0.9	4	16	36	16	48	0
$\bar{\Sigma}^+\Sigma^-$	1.0 ± 5.4	1.0	0.1 ± 0.5	0	100	0	36	0	0
$\bar{\Sigma}^0\Lambda$+c.c.	66 ± 13	1.12	5.8 ± 1.1	6	6	6	6	8	0
$\bar{\Sigma}^0\Sigma^0$	<15	1.0	<1.5	1	49	9	25	12	0

[a] Test $= \dfrac{1.23}{\text{Phase space}} \times \dfrac{\sigma(\mu b)}{113} \times 9$.

Treating all events as ambiguous between a Λ and Σ^0 at the production vertex, the cross sections can best be summarized as follows:

$$\sigma[\bar{p}+p \to \Lambda(\text{or }\Sigma^0)+\bar{\Sigma}^-+\pi^++\text{c.c.}]=28.8\pm10.5 \ \mu b,$$

$$\sigma[\bar{p}+p \to \Lambda(\text{or }\Sigma^0)+\bar{\Sigma}^++\pi^-+\text{c.c.}]=10.3\pm 4.7 \ \mu b.$$

Estimates based on the best assignment for each event gave the following breakdown of these cross sections (this breakdown may be seriously biased):

$$\bar{p}+p \to \Lambda+\bar{\Sigma}^-+\pi^++\text{c.c.} \quad 25.9\pm10.1 \ \mu b,$$

$$\bar{p}+p \to \Lambda+\bar{\Sigma}^++\pi^-+\text{c.c.} \quad 6.6\pm 3.9 \ \mu b,$$

$$\bar{p}+p \to \Sigma^0+\bar{\Sigma}^-+\pi^++\text{c.c.} \quad 2.9\pm 2.9 \ \mu b \ (\text{one event}),$$

$$\bar{p}+p \to \Sigma^0+\bar{\Sigma}^++\pi^-+\text{c.c.} \quad 3.7\pm 2.6 \ \mu b.$$

These cross sections are much lower than the equivalent cross sections at higher incident momenta (Fig. 11b) because the center-of-mass energy of this experiment is close to reaction threshold.

One event has been observed for the reaction $\bar{p}p \to \Lambda^0 K^+ \bar{p}$ corresponding to a cross section of $2.3\pm2.3 \ \mu b$.

Finally all combinations of particles having the same sets of quantum numbers for strangeness, baryon number, and charge when examined together showed no indication of Y^* production within the limited statistics.

VII. FOUR-BODY FINAL STATES

Because the total energy in the c.m. system is 2670 MeV and the thresohld energy of a $\bar{\Lambda}\Lambda\pi^0\pi^0$ final state is 2500 MeV, it is expected that the cross sections for $\bar{Y}Y\pi\pi$ final states are very small. Two events of the reaction $\bar{p}p \to \bar{\Lambda}\Lambda\pi^+\pi^-$ have been observed corresponding to a cross section of $3\pm2 \ \mu b$. No other $\bar{Y}Y\pi\pi$ final states have been observed.

VIII. CONCLUSIONS

We have measured the cross sections for hyperon production near threshold in 2.7 GeV/c $\bar{p}p$ interactions. These cross sections (Table II) are compared with the values reported at other energies[1–5] in Fig. 11. Roy[10] has predicted the s dependence of the total cross sections for the two-body final states using the $K^*(888)$ Regge pole in the t channel. This prediction is compared with the experimental data in Fig. 11, although this model is not expected to behave well below 3 GeV/c ($s=7.67$

GeV²) where poles other than the $K^*(888)$, such as $K^*(1400)$, may be needed. In Fig. 11(a), the $\bar{\Lambda}\Lambda$ cross section appears to go through a maximum near $s=7$ GeV² (for this experiment $s=7.1$ GeV²). The s dependence of the $\bar{\Sigma}^-\Sigma^+$ cross section is much flatter than predicted by Roy.

The branching ratios among the interactions $\bar{p}p \to \bar{Y}Y$ may be used as a test of SU_3. Tanaka[21] has given a Table of SU_3 coefficients coupling $\bar{p}p$ to $\bar{Y}Y$ through the t channel. Our data, summarized in Table III along with the squares of the coefficients given by Tanaka,[21] are consistent with the exchange of a pure antisymmetric octet in the cross channel (t channel) as would be expected for the exchange of K or K^* mesons. In a similar way, Chien et al.[5] have compared the data of 3.0, 3.25, 3.6, 3.7, 4.0, and 6.9 GeV/c incident antiproton momentum finding good agreement in all cases with Tanaka's antisymmetric octet coefficients.

Coupling of $\bar{p}p$ to $\bar{Y}Y$ is probably large through the t channel and small through the s channel because the interaction is strongly peripheral and because $\bar{\Sigma}^+\Sigma^-$ production is small.

In the three-body final states there is little evidence of Y^* production, maybe because there is little energy available above threshold.

The t dependence of the differential cross section $\bar{p}p \to \bar{\Lambda}\Lambda$ is fitted quite well by the absorption models of Högaasen and Högaasen[12] and Iddings and Marshall[13] as shown in Figs. 3 and 5, respectively. The forward peak is also satisfactorily fit by a reaction model with a disc of radius 1.3 F which is about equal to the $\bar{p}p$ elastic interaction radius at this energy.

[21] K. Tanaka, Phys. Rev. 135, B1186 (1964).